MNRAS **000**, 1–5 (2020) Preprint 20 May 2020 Compiled using MNRAS LATEX style file v3.0

Tidal Effects and Post-Main Sequence Orbital Dynamics

Stanley A. Baronett,[1]★ Daniel Tamayo,[2]† Noah Ferich,[3]‡ Jason H. Steffen,[1]§
[1]*Department of Physics & Astronomy, University of Nevada, Las Vegas, 4505 S. Maryland Pkwy, Las Vegas 89154, USA*
[2]*Department of Astrophysical Sciences, Princeton University, Princeton, NJ 08544, USA*
[3]*Department of Astrophysical & Planetary Sciences, University of Colorado Boulder, Boulder, CO 80309, USA*

ABSTRACT
By introducing new code into REBOUNDx and techniques to interpolate stellar data from MESA, we investigated the evolution of the solar system's orbital dynamics during the Sun's post-main sequence mass loss. Preliminary unit-test results indicate that the Earth may survive the tip of the red-giant branch phase, but, in agreement with findings among existing literature, the Sun will likely engulf Mercury and Venus beforehand. We further investigated the dissipative effects of tidal interactions between a highly-evolved and slowly-rotating red-giant Sun and any nearby bodies, e.g., the Earth. In doing so, we contributed additional new code to model the effect in REBOUNDx. These REBOUNDx additions are publicly available in software's latest releases and can be applied to a variety of dynamical investigations, including instability timescales for exoplanet systems and sources of white dwarf pollution.

Key words: planet–star interactions – Sun: evolution – *(Sun:)* solar wind – software: development – software: simulations – software: public release

1 INTRODUCTION

The eventual fate of our solar system, as our Sun evolves through the rest of its post-main sequence (MS) phases to become a white dwarf (WD), has been investigated to various extents over several decades. For example, studies into the effects on Earth's atmosphere from distant yet gradual heating include Sackmann, Boothroyd & Kraemer (1993), Rybicki & Denis (2001), Schröder, Smith & Apps (2001), and Laughlin (2007). But conclusions as to whether Earth at all survives the Sun's journey to becoming a WD—in particular through its red-giant branch (RBG) phase—are not well in agreement.

Schröder & Smith (2008), and some general textbooks, e.g., Prialnik (2000), p. 10, contend Earth will be engulfed by the tip of the RGB (TRGB) phase. Meanwhile others, e.g., Schröder et al. (2001), argue for Earth's survival and even for Venus' (Sackmann et al. 1993). However, most agree that if the Sun's significant mass loss during its RGB phase is ignored, and the planetary orbits do *not* adiabatically expand, then the Earth and perhaps Mars would likely be engulfed by the tip of the later asymptotic giant branch (AGB), as the solar radius may swell to over an AU (astronomical unit).

Thus, one deciding factor in the planets' fates hinges on the rate at which the Sun is expected to lose mass. Another, as we will come to discuss, involves the dissipative effects of tidal interactions between a slowly rotating star and a nearby orbiting body. In what follows, we analyze the contributions of each of these considerations by using data from Modules for Experiments in Stellar Astrophysics (MESA) and simulations with our recent additions to REBOUNDx, an extended library for the N-body integrator REBOUND.

2 SOLAR MASS LOSS

2.1 MESA

We employed Modules for Experiments in Stellar Astrophysics (MESA Paxton et al. 2011, 2013, 2015, 2018, 2019), a fast, open-source, modular, 1D stellar evolution code,[1] to model the Sun from pre-MS to WD given default initial values (e.g., stellar mass and metallicity) as provided in its existing test suite for a $1M_\odot$ star. Some advantages of MESA over other stellar evolution codes is its comprehensive microphysics and detailed chemistry which can account for sophisticated chemical compositions beyond simple Z values (metallicity). Of critical importance to our investigation are the program's advanced options for mass loss through stellar winds.

MESA executes mass loss adjustments at each timestep, before solving the stellar structure and composition equations, and supports various preloaded (as well as custom) mass-loss rate configurations along different evolutionary stages (Paxton et al. 2011, p. 16). For

★ E-mail: barons2@unlv.nevada.edu
† NHFP Sagan Fellow: dtamayo@astro.princeton.edu
‡ E-mail: noah.ferich@colorado.edu
§ E-mail: jason.steffen@unlv.edu

[1] MESA is freely available at http://mesa.sourceforge.net/.

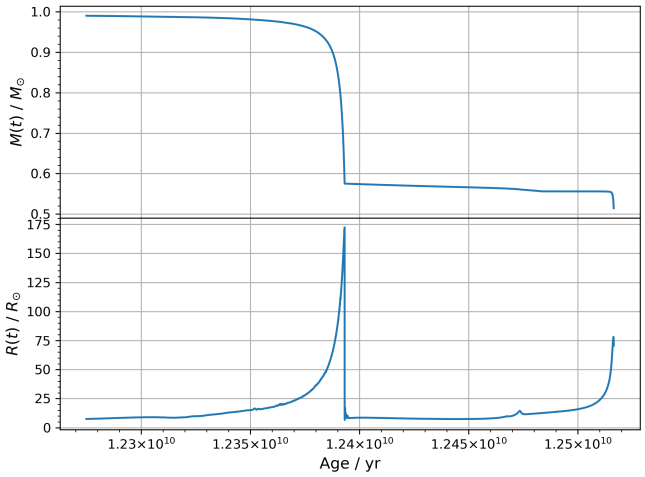

Figure 1. MESA results of post-main sequence stellar mass (top) and radius (bottom) evolution during the RGB and AGB phases for a 1 $M_\odot$ star. For reference, 1 AU $\approx 215 R_\odot$.

the RGB in particular, we implemented the well-known Reimers (1975) formula for MESA's "cool-wind RGB scheme," namely

$$\dot{M} = 4 \times 10^{-13} \eta \frac{L_* R_*}{M_*}, \tag{1}$$

where L_*, R_*, and M_* respectively are the stellar luminosity, radius, and mass, all in solar units; and η is a dimensionless scaling factor.

Depending on specific or relevant observational data, Reimers' empirically-derived relationship allows some flexibility in choosing an appropriate value for η to accommodate somewhat lower or higher mass-loss rates, e.g., $0.3 < \eta < 3$ (Lamers & Cassinelli 1996, p. 168). But this flexibility in the parameter η also lends itself to considerable uncertainty, as highlighted in both Schröder & Smith (2008) and Veras & Wyatt (2012). We opted to maintain the test suite's default factor of $\eta = 0.8$, which falls within a reasonable range for the Sun ($0.4 < \eta < 0.8$), according to Sackmann et al. (1993), and as discussed in Veras & Wyatt (2012, p. 2970).

Running the MESA simulation produces a comprehensive and configurable "history" file which includes time-series data of various stellar properties as a function of age. Plotted in Fig. 1 are the post-MS results for the mass and radius of a $1 M_\odot$ star (e.g., the Sun) as a function of its age, until the end of the AGB phase. In the top plot, note the Sun's gradual, then rapid, mass loss along the RGB phase, losing more than 2/5 its initial mass by TRGB. A similar trend can be seen along the AGB, although the loss-rate remains mostly constant until the TAGB, when the Sun begins entering its WD phase with roughly half its MS mass.

In the bottom plot, note the corresponding, rapid, radial expansion, driven by increased fusion energy (CNO cycle) in its hydrogen shells, during its RGB phase. The Sun's radius grows by almost a factor of 175 by the TRGB (for reference, 1 AU $\approx 215 R_\odot$). Afterwards, we can see some indications of thermal pulses along the AGB, which correspond to drops in mass, leading up to its respective TAGB. With this data in hand, the next step was to study how the solar system might evolve given these dramatic changes.

2.2 REBOUND and REBOUNDx

To simulate the orbital dynamics of the planets, we used REBOUND[2], a flexible and customizable N-body integrator, featuring several high order and high accuracy, symplectic and non-symplectic, integration schemes with adaptive or fixed timesteps (Rein & Liu 2012). Although one could manually set a particle's mass between timesteps out-of-the-box in REBOUND, there was no way to input or update a particle's parameter values based on existing time-series data. More advanced mass modifications requires REBOUNDx (eXtras),[3] an extended library for REBOUND that allows implementation of additional, conservative and dissipative, physical effects, e.g., general relativity or radiation forces (Tamayo et al. 2020). However, at the time, the only mass-modification option available was restricted to a particle's exponential loss or gain, adjustable by a single `tau_mass` parameter, i.e., the e-folding timescale (Kostov et al. 2016). Therefore more complicated or non-smooth mass loss functions, such as the mass profile in Fig. 1, could not be properly accounted for by this particular existing "additional effect."

In order for a REBOUND simulation and its particles to be informed of the mass-profile data from MESA at each timestep, we wrote custom code to accomplish the following: (1) load a time-series, parameter-data file and store its values in the simulation's allocated memory; and (2) spline the discrete dataset so REBOUND could interpolate a parameter's value at any arbitrary timestep in the simulation. For the latter objective we chose to employ a cubic spline. Aside from being the most popular of the splines, its resulting interpolant remains continuous through its second derivative, allowing flexible handling of boundary conditions, i.e., the endpoints of the dataset. In general, splines, which are piecewise polynomials, suffer less from Runge's phenomenon (i.e., wild oscillation around sharp corners or rapidly changing higher derivatives) than do polynomial interpolations. This stability is essential for meaningful interpolation of the non-smooth MESA data, particularly around the tips of the RGB and AGB (see Fig. 1).

Working with REBOUNDx's primary developer, Daniel Tamayo, we contributed our "Parameter Interpolation" code for inclusion in a publicly released version (3.1.0).[4] To ensure machine independence and avoid REBOUNDx requiring additional libraries or dependencies, we introduced spline and interpolation functions to the code from scratch, adapting the cubic spline algorithm from Press et al. (1992). REBOUNDx now accepts a pair of arrays—one a monotonically non-decreasing time series, and the other a series of parameter values in one-to-one correspondence—whose values can come from any data file, MESA or otherwise. We additionally incorporated an optimized searching algorithm[5] to efficiently traverse the time-series data (as is naturally done by the simulation's advancing timestep) for proper interpolation. This makes the code robust enough to support forward and backward integrations, as well as arbitrary or random spline interpolation calls.

2.3 Unit Test Results

As a preliminary test and proof of concept, we simulated an idealized Sun-Earth system roughly 4 million years (Myr) before the

[2] REBOUND is freely available at http://github.com/hannorein/rebound.
[3] REBOUNDx is freely available at https://github.com/dtamayo/reboundx.
[4] reboundx.readthedocs.io/en/latest/effects.html#parameter-interpolation
[5] If the time-series data is truly monotonic, the algorithm, on average, performs in constant time, i.e., $O(1)$.

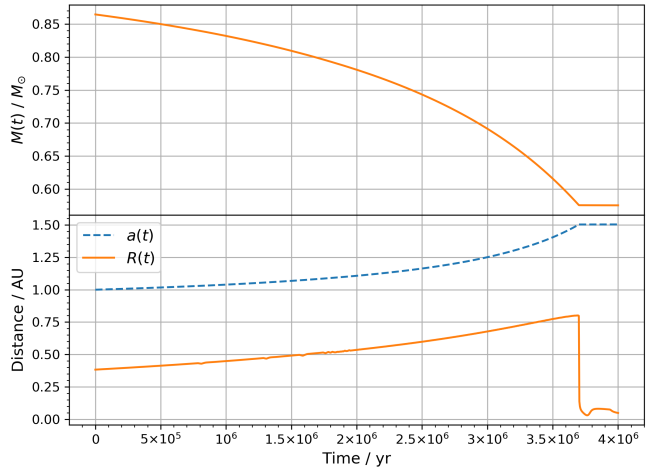

Figure 2. Simulated evolution of the Sun's mass and radius (orange solid curves), and Earth's semi-major axis (blue dashed curve), for approximately 4 million years before the tip of the RGB phase. In this test, Earth's orbital radius started exactly at 1 AU.

TRGB.[6] We invoked our new "Parameter Interpolation" code in REBOUNDx to load in the Sun's historical MESA data and interpolate both its mass and radius at each timestep. Note that, in this exhibitive test, Earth's initial semi-major axis, $a_\oplus(t = 0)$, is 1 AU. Since the Sun will lose substantial mass throughout its RGB phase, a more complete simulation should find Earth's orbit to have adiabatically expanded beyond 1 AU before the start of this test. Because the entire simulation integrates millions of orbits, we elected to use REBOUND's WHFAST integrator, based on the second-order Wisdom-Holman scheme with up to 11$^{\text{th}}$-order symplectic correctors to reduce the energy error over long timescales (Rein & Tamayo 2015).

Plotted in Fig. 2 are the Sun's mass and radius, and Earth's semi-major axis, as a function of simulation time. Notice this mass profile corresponds to a smaller, 4 Myr limited range of that seen in Fig. 1. As we physically expect, Earth's orbit adiabatically expands, in sync with the Sun's mass loss, stopping at about 1.5 AU when TRGB is reached and rapid mass loss halts for most of the AGB. Notice also that, in this test, the Earth well avoids being engulfed by a Sun whose radius reaches at most 0.8 AU; this is despite the substantial "handicap" given to the Sun by starting Earth at 1 AU this close to TRGB. That being said, both Mercury and Venus (the latter's perihelion is $\sim$ 0.72 AU) will not likely survive the RGB phase, in accordance with the existing literature on the subject.

3 CLOSE-ENCOUNTER TIDAL INTERACTIONS

3.1 Theory and Implementation

Although the Sun will most likely clear the inner planets (e.g., Mercury and Venus) along its relatively fast ascent of the RGB, the solar photosphere may come quite close to the Earth's orbit depending on the mass-loss rate model used or the value of η in Reimers formula. At separation distances, between the photosphere and Earth, of just a few tenths of an AU, Schröder & Smith (2008) finds the loss of Earth's angular momentum due to tidal interactions to not only be substantial but, by their calculations, fatal. We therefore found this non-conservative effect due to tides worth investigating.

Post-MS magnetic braking on an immensely inflated red giant will cause the Sun to virtually stop rotating after about 2 billion years (Schröder & Smith 2008, §1). As such, any closely orbiting body will experience a continuous drag from retarded tidal bulges on the photosphere. Investigations into the equilibrium tide of close binary stars in Zahn (1977, 1989) showed that tidal friction in the outer convection envelope of the red giant causes a retardation in the tidal bulges. Assuming a circular orbit and uniform solar rotation, the tidal torque on the nearby Earth is given by (Zahn 1989, Eq. 11):

$$\Gamma = 6\frac{\lambda_2}{t_f} q^2 M R^2 \left(\frac{R}{r_\oplus}\right)^6 (\Omega - \omega), \tag{2}$$

where M, R, and Ω respectively are the mass, radius, and rotational angular velocity of the Sun; $q = m_\oplus/M(t)$ is the mass ratio, $r_\oplus$ is the distance between the Sun's and Earth's centers of mass, and ω is Earth's orbital angular velocity. λ_2 depends on properties of the convective envelope, and $t_f\,(t) = (M(t)R(t)^2/L(t))^{1/3} \approx O(1\text{yr})$ is the convective friction time (Zahn 1989, Eq. 7).

At the time, REBOUNDx supported only one additional effect for tides raised on interacting bodies, but it was specific to the instantaneous equilibrium case, resulting only in orbital precession from a conservative, radial, non-Keplerian potential. Therefore to observe the dissipative tidal drag interaction between the RGB Sun and Earth in our REBOUND simulations, we wrote, added, and tested a custom REBOUNDx effect by first implementing Eq. 2.

Daniel Tamayo later helped to contribute this additional effect to the main REBOUNDx code. Since valid applications of Eq. 2 are restricted to circular orbits, Tamayo instead implemented a general form of the weak friction model for tidal interaction in binary systems with constant time lag. In particular, he followed Hut (1981, Eq. 8):

$$\boldsymbol{F} = -G\frac{Mm}{r^2}\left\{\hat{r} + 3q\left(\frac{R}{r}\right)^5 k_1\left[\left(1 + 3\frac{\dot{r}}{r}\tau\right)\hat{r} - (\Omega - \dot{\theta})\tau\hat{\theta}\right]\right\}, \tag{3}$$

where k_1 is the apsidal motion constant of the primary body (equal to half the tidal Love number k_2[7]), and τ is a small constant time lag that corresponds to the slight change in both amplitude and direction (i.e., misalignment) of the tides, introducing dissipation to the system; $\tau = 0$ corresponds to the case of instantaneous equilibrium tides. The azimuthal component of Eq. 3 has the same functional form as Eq. 2. And since this formula also includes a radial component, it can also work for eccentric orbits. The final implementation of this effect[8] was included in a publicly released version (3.0.5) of REBOUNDx.

3.2 Unit Test Setup and Results

By importing and interpolating MESA data (using the techniques laid out in § 2.2), the values of M, R, and Ω can be easily retrieved at each timestep. Since MESA's values for Ω near the end of the RGB are on the order of 10^{-9} or smaller, for calculational simplicity we assumed $\Omega = 0$ in our tests. Following Schröder & Smith (2008, §4.1), we assumed a fully convective envelope (Zahn 1989, Eq.

[6] A Jupyter Notebook example of this interpolation test can be found here.

[7] The Love number k_2 is defined as the cubical dilation: the ratio of the additional potential, from the self-reactive force (produced by the deformation), to the deforming potential, or $kV\,(\theta, \phi)/g$. For rigid bodies, $k_2 = 0$.

[8] reboundx.readthedocs.io/en/latest/effects.html#tides-constant-time-lag

15) and tidal period of 1 year by fixing $\lambda_2 \approx 0.019\alpha^{4/3} \approx 0.038$, where $\alpha \approx 1.7$ is a coefficient convection parameter. As Schröder & Smith (2008) notes, simplifications to the mixing length theory have introduced a source of uncertainty in α.

Although t_f in Eq. 2 can be easily calculated, the final version's implementation of Eq. 3 instead requires a determination of k_1 and τ in terms of Zahn's parameters, instead. According to Zahn (1989, 1977), λ_2 is approximately equal to k_1. With this equivalence, by setting Eq. 2 equal to the azimuthal ($\hat{\theta}$) component of Eq. 3 and solving for τ, we arrived at

$$\tau = \frac{2R^3 r}{GMt_f}. \tag{4}$$

In the results of the unit test that follows, we again set up an idealized Sun-Earth system slightly before the TRGB. However, since the test using MESA data in § 2.3 shows the solar radius never coming within less than 0.5 AU of Earth's orbit (see Fig. 2), this simulation's setup is more contrived in order to demonstrate the effect of the dissipative tidal interaction. As such, for the entirety of the relatively short simulation, $M = 0.86M_\odot$, $R = 0.85R_\odot$, and $m_\oplus = 3 \times 10^{-6} M_\odot$ all remain constant throughout. Earth's initial semi-major axis and eccentricity respectively begin with $a_\oplus = 1$ AU and $e_\oplus = 0.03$. We additionally fixed $\lambda_2 = k_1 = 0.03$ (as just mentioned) and set $\tau = 0.4$ by substituting the aforementioned constants into Eq. 4.[9]

We used one of the tidal evolution equations derived in Hut (1981, Eq. 9) to predict the decay of Earth's orbit as a function of time, allowing for a direct comparison with the results of the newly implemented REBOUNDx effect. The evolution equation in particular is

$$\frac{da}{dt} = -6\frac{k_1}{T} q(1+q) \left(\frac{R}{a}\right)^8 \frac{a}{(1-e^2)^{15/2}} \cdot \left\{ f_1(e^2) - (1-e^2)^{3/2} f_2(e^2) \frac{\Omega}{n} \right\}, \tag{5}$$

where

$$f_1(e^2) = 1 + \tfrac{31}{2}e^2 + \tfrac{255}{8}e^4 + \tfrac{185}{16}e^6 + \tfrac{25}{64}e^8,$$
$$f_2(e^2) = 1 + \tfrac{15}{2}e^2 + \tfrac{45}{8}e^4 + \tfrac{5}{16}e^6,$$

$n = G^{1/2}(M+m)^{1/2}a^{-3/2}$ is the mean orbital angular velocity, and

$$T = \frac{R^3}{GM\tau}$$

"is a typical time scale on which significant changes in the orbit take place through tidal evolution" (Hut 1981, p. 128). Since Earth's eccentricity is quite small in the simulation (0.03), we assumed a circular orbit, i.e., $e = 0$. Finally, solving the differential Eq. 5 yields a predictive expression for Earth's semi-major axis as a function of time, namely

$$a(t) = R\left[\left(\frac{a_0}{R}\right)^8 - 48\frac{k_1}{T} q(1+q)t\right]^{1/8}. \tag{6}$$

The REBOUNDx, unit-test results of a 25,000 year integration are plotted in Fig. 3.[10] We see that the new effect causes Earth's orbit to decay into the "surface" of the Sun, as expected. Plotted for comparison is the theoretical decay predicted by Eq. 6. Given the relatively short timescale of the simulation, we chose the computationally more expensive, but more accurate, default "Implicit integrator with Adaptive timeStepping, 15th order" (IAS15), which can maintain high precision even in the presence of velocity-dependent forces (Rein & Spiegel 2015), to more accurately compare with our theoretical prediction. The increasing, but minor, difference between the simulated and actual $a(t)$ stems from the discrepancy between the aforementioned simulated and predicted eccentricities.

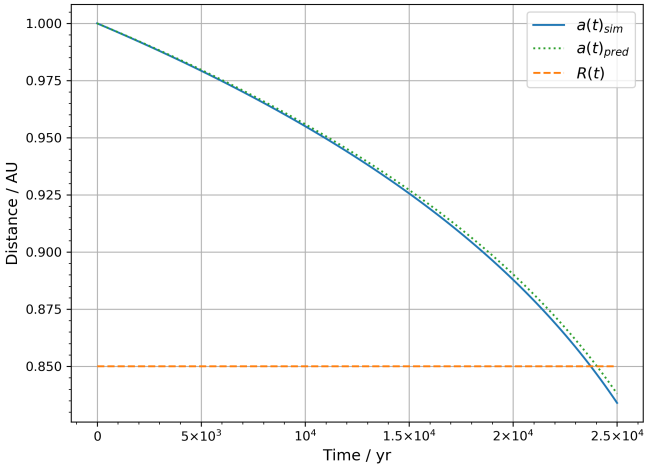

Figure 3. 25,000-year simulation of the Earth's orbital decay and engulfment due to dissipative tidal interactions with the Sun. $a(t)_{\rm sim}$ and $a(t)_{\rm pred}$ respectively are the simulated (solid blue) and predicted (dotted green) evolutions of Earth's semi-major axis. The solar radius (dashed orange) $R(t) = 0.85$ throughout.

4 CONCLUSIONS

Although Earth appears to survive the idealized test in §2.3, a more thorough investigation and confident determination of the matter should include fully n-body dynamical simulations of all the planets over much longer, post-MS timescales (e.g., at least hundreds of millions of years). More attention to the Sun's mass-loss rate is also needed, whether it be calibrating Reimers' scaling factor η, based on observational data, or perhaps substituting for existing refinements to Reimers formula found in the literature, e.g., Schröder & Cuntz (2005, Eq. 4).

Further insight into the mechanisms and accuracy of engulfment during any close-encounter tidal interactions requires a more comprehensive understanding of the Sun's "radius," typically defined as the radius to where the optical depth in the photosphere reaches 2/3. Finally, other arenas worth exploring with the new additions to REBOUNDx include timescales for instabilities among various observed exoplanet systems, as well as with asteroids during the WD phase. For the latter in particular, this new code could help better investigate resonance breaking and scattering of asteroids (e.g., WD pollution).

ACKNOWLEDGEMENTS

The authors thank the referee for constructive comments that improved this manuscript.

[9] Note: the units of the REBOUND simulations are in years, AU, and $M_\odot$. Therefore $G = 4\pi^2$ AU$^3 \cdot$ yr$^{-2} \cdot M^{-1}$.

[10] A Jupyter Notebook example of this tidal test can be found here.

REFERENCES

Hut P., 1981, A&A, 99, 126
Kostov V. B., Moore K., Tamayo D., Jayawardhana R., Rinehart S. A., 2016, ApJ, 832, 183
Lamers H. J. G. L. M., Cassinelli I. P., 1996, Mass Loss from Stars. Astronomical Society of the Pacific, p. 162
Laughlin G. P., 2007, Sky & Telescope, June issue, 32
Paxton B., Bildsten L., Dotter A., Herwig F., Lesaffre P., Timmes F., 2011, ApJS, 192, 3
Paxton B., et al., 2013, ApJS, 208, 4
Paxton B., et al., 2015, ApJS, 220, 15
Paxton B., et al., 2018, ApJS, 234, 34
Paxton B., et al., 2019, ApJS, 243, 10
Press W. H., Teukolsky S. A., Vetterling W. T., Flannery B. P., 1992, Numerical recipes in C. The art of scientific computing. Cambridge Univ. Press
Prialnik D., 2000, An Introduction to the Theory of Stellar Structure and Evolution. Cambridge Univ. Press, Cambridge
Reimers D., 1975, Memoires of the Societe Royale des Sciences de Liege, 8, 369
Rein H., Liu S. F., 2012, A&A, 537, A128
Rein H., Spiegel D. S., 2015, MNRAS, 446, 1424
Rein H., Tamayo D., 2015, MNRAS, 452, 376
Rybicki K. R., Denis C., 2001, Icarus, 151, 130
Sackmann I.-J., Boothroyd A. I., Kraemer K. E., 1993, ApJ, 418, 457
Schröder K. P., Cuntz M., 2005, ApJ, 630, L73
Schröder K.-P., Smith R. C., 2008, MNRAS, 386, 155
Schröder K.-P., Smith R. C., Apps K., 2001, A&G, 42, 6.26
Tamayo D., Rein H., Shi P., Hernand ez D. M., 2020, MNRAS, 491, 2885
Veras D., Wyatt M. C., 2012, Monthly Notices of the Royal Astronomical Society, 421, 2969
Zahn J. P., 1977, A&A, 500, 121
Zahn J. P., 1989, A&A, 220, 112

This paper has been typeset from a TEX/LATEX file prepared by the author.